7854 *Biochemistry* **2010,** *49,* 7854–7866
DOI: 10.1021/bi1008408

BIOCHEMISTRY
including biophysical chemistry & molecular biology
*Article*

# Modeling of the Endosomolytic Activity of HA2-TAT Peptides with Red Blood Cells and Ghosts[†]

Ya-Jung Lee, Gregory Johnson, and Jean-Philippe Pellois*

*Department of Biochemistry and Biophysics, Texas A&M University, College Station, Texas 77843*

*Received May 25, 2010; Revised Manuscript Received August 11, 2010*

ABSTRACT: HA2-TAT is a peptide-based delivery agent that combines the pH-sensitive HA2 fusion peptide from influenza and the cell-penetrating peptide TAT from HIV. This chimeric peptide is engineered to induce the cellular uptake of macromolecules into endosomes via the TAT moiety and to respond to the acidifying lumen of endosomes to cause membrane leakage and release of macromolecules into cells via the HA2 moiety. The question of how HA2 and TAT affect the properties of one another remains, however, unanswered, and the behavior of the peptide inside endosomes is mostly uncharacterized. To address these issues, the binding and membrane leakage activity of a glutamic acid-enriched analogue E5-TAT was assessed with red blood cells and giant unilamellar vesicles as membrane models for endosomes. Hemolysis and microscopy assays reveal that E5-TAT binds to membranes in a pH-dependent manner and causes membrane leakage by inducing the formation of pores through which macromolecules can escape. The TAT moiety contributes to this activity by causing a shift in the pH response of E5 and by binding to negatively charged phospholipids. On the other hand, TAT binding to glycosaminoglycans reduces the lytic activity of E5-TAT. Addition of TAT to the C-terminus of E5 can therefore either increase or inhibit the activity of E5 depending on the cellular components present at the membrane. Taken together, these results suggest a model for the endosomolytic activity of the peptide and provide the basis for the molecular design of future delivery agents.

Cell-penetrating peptides (CPPs)[1] provide general and useful tools to deliver macromolecular cargos into live cells. A prototypical CPP is the TAT peptide derived from HIV TAT (*1*, *2*). TAT has been used to deliver peptides, proteins, DNA, liposomes, and nanoparticles (*3*, *4*). Multiple mechanisms are involved in cellular penetration mediated by TAT. TAT has been shown to directly translocate across the lipid bilayer of the plasma membrane when it is both labeled with a small molecule and present above a threshold concentration (*5*). On the other hand, TAT is internalized by endocytosis at low concentration or when conjugated to large hydrophilic molecules (*6*). Multiple endocytic mechanisms have been shown to be involved in the uptake of TAT conjugates. TAT conjugates can for instance enter cells by clathrin- or caveolin-dependent endocytosis. In addition, TAT and other CPPs have also been shown to induce macropinocytosis, an effect that leads to the increase in uptake of fluid-phase endocytosis markers (*6*−*8*). Induction of macropinocytosis appears to be mediated by the interaction of the positively charged peptide with membrane-associated heparan sulfate proteoglycans (*9*). However, recent evidence suggests that HSPG do not act as receptors but rather might act as a binding reservoir for TAT and that other proteins might be involved in the induction of macropinocytosis (*10*). Following internalization, TAT is able to promote the escape of its cargo from the lumen of endosomes into the cell cytosol. This second step in the delivery process remains poorly understood, yet it is often critical for the successful delivery of bioactive macromolecules into cells. For instance, macromolecules targeted to the cell nucleus or other cellular organelles first have to be released into the cytosolic space before they can reach their intended site of action. A major problem with TAT and other TAT-like CPPs however is that endosomal escape is not efficient and a large fraction of the internalized macromolecules remains trapped inside endocytic organelles (*11*). The macromolecules, during their transit from early to late endosomes and to lysosomes, are then subjected to degradation (*11*, *12*). In order to improve the endosomolytic activity and the delivery efficiency of TAT, one strategy consists of adding peptides that can lyse lipid bilayers at acidic pH (*13*). This is based on the principle that such peptides might become activated during trafficking in the endocytic pathway as the vacuolar $H^+$-ATPase acidifies the lumen of endocytic organelles (*14*). As a result, lysis of endosomal membrane might be achieved without causing lysis of the plasma membrane or other membraneous organelles. This pH-dependent selectivity is therefore important to maintain low cytotoxicity of the delivery peptide. An example of pH-dependent lytic peptide is the HA2 fusion peptide (*15*). HA2 is a peptide derived from the hemagglutinin protein of Influenza, a virus that relies on endosomal acidification to successfully deliver its nucleic acid content to host cells (*16*). HA2 and HA2 mutants has been extensively studied and shown to have both membrane fusion and lysis

[†]This work was supported by Award Number R01GM087227 from the National Institute of General Medical Sciences. G.J. was partially supported by a NIH molecular biophysics training grant (T32GM065088).

*To whom correspondence should be addressed. Phone: 979 845 0101. Fax: 979 862 4718. E-mail: pellois@tamu.edu.

[1]Abbreviations: CPP, cell-penetrating peptide; RBCs, red blood cells; Fl, fluorescein isothiocyanate; Ahx, 6-aminohexanoic acid; PS, phosphatidylserine; GUVs, giant unilamellar vesicles; DPPC, 1,2-dipalmitoyl-*sn*-glycero-3-phosphocholine; SM, sphingomyelin; DPPS, 1,2-dipalmitoyl-*sn*-glycero-3-phospho-L-serine; TMR, 5(6)-carboxytetramethylrhodamine; HS, heparan sulfate; HSPG, heparan sulfate proteoglycans; LBPA, lysobisphosphatidic acid; PBS, phosphate saline buffer; DMSO, dimethyl sulfoxide; HEPES, 4-(2-hydroxyethyl)-1-piperazineethanesulfonic acid.

 Published on Web 08/13/2010 

Table 1: Sequences of the HA2-TAT Peptides Investigated

| name | amino acid sequence |
|---|---|
| HIV TAT (48−57) | GRKKR RQRRR |
| influenza HA2 (1−23) | GLFGA IAGFI ENGWE GMIDG WYG |
| E3-TAT[a] | GLFGA IAGFI ENGWE GLIEG WYGGR KKRRQ RRR |
| E5-TAT[a] | GLFEA IAEFI ENGWE GLIEG WYGGR KKRRQ RRR |
| Fl-E5-TAT[b] | Fl-Ahx-GLFEA IAEFI ENGWE GLIEG WYGGR KKRRQ RRRK |
| E5-TAT-Fl | GLFEA IAEFI ENGWE GLIEG WYGGR KKRRQ RRRK(εFl) |
| E5(3,7)-TAT | GLEGA IEGFI ENGWE GLIEG WYGGR KKRRQ RRR |
| E5-R9 | GLFEA IAEFI ENGWE GLIEG WYGGR RRRRR RRR |

[a]The underlined sequence represents the HA2 peptide obtained after trypsin digest. [b]Ahx is the linker 6-aminohexanoic acid.

activities (*15*, *17*). The pH-dependent lysis activity is related to the ability of the peptide to insert into lipid bilayers upon protonation of glutamate residues. HA2-derived peptides have been used to enhance the endosomal release and delivery of DNA particles (*18*, *19*). HA2 analogues have also been used to transiently permeabilize the plasma membrane of live cells to achieve cytosolic transfer of oligonucleotides (*20*). More recently, HA2 has been fused to TAT and used as an additive that could enhance the delivery of proteins labeled with TAT (*6*). The rationale is that HA2-TAT and a TAT-protein conjugate might accumulate together in endocytic organelles because both species contain TAT and that HA2-TAT might assist the TAT-protein in its endosomal escape. Recently, we have shown that this principle could be extended to macromolecules not labeled with TAT as peptides derived from HA2-TAT were able to stimulate both macropinocytosis and endosomal release of macromolecules present in the cell culture media (*21*). Finally, HA2-TAT has also been used for the delivery of quantum dots into cardiac myocytes (*22*). While these reports highlight the usefulness of HA2 conjugated to CPPs for cell culture applications, the potential value of this type of reagent has also been demonstrated in the context of therapeutic applications. HA2 has, for instance, also been fused to the N-terminus of the tumor suppressor p53 modified with the CPP R11, and the formed HA2-p53-R11 construct was shown to reduce the proliferation of cancer cells more efficiently than p53-R11 alone (*23*).

Despite the progress that has been made in understanding the mechanisms by which TAT or HA2 function, little is known about how these peptides mediate endosomal release of macromolecules. This is in part because it is difficult to investigate this particular step in a complex cellular environment in which many other processes take place. In addition, simpler but more controllable lipid bilayer models such as liposomes often fail to reproduce the peptide activities observed in cells. For instance, while TAT penetrates cells, it does not typically cross the lipid bilayer of liposomes (*24*, *25*). It has been suggested that the membrane potential and phospholipid asymmetry of biological bilayers are key determinants for the translocation activity of TAT. Yet, these membrane properties cannot be easily reproduced in liposomes. In the case of HA2, the lysis of liposomes does not always display the pH dependence observed with biological membranes (*26*). The reasons for this remain unclear, but assays with liposomes are typically complicated by the fact that HA2 might promote both fusion and lysis. On the other hand, HA2's pH-dependent lysis activity can be readily demonstrated by the hemolysis of red blood cells (RBCs) (*15*). In this report, we investigate the lytic properties of HA2-TAT and of related peptides with red blood cells. We show that TAT has a dual effect on the activity of HA2 peptides, both inhibiting and enhancing their lytic activities depending on the environment. In turn, the activity of HA2-TAT peptides is highly dependent on pH but also on the presence of glycoaminoglycans, on phospholipid composition, and on peptide concentration. These studies reveal valuable mechanistic insights on how these CPPs might cause endosomal lysis and provide a basis for the design of optimized delivery agents.

## EXPERIMENTAL PROCEDURES

*Peptide Synthesis and Purification*. E3-TAT, E5-TAT, Fl-E5-TAT, E5-TAT-Fl, E5(3,7)-TAT, and E5-R9 were purchased as crude cleavage products from RayBiotech (Norcross, GA). Peptide sequences are described in Table 1. TAT and TMR-TAT were synthesized in-house on the Rink amide resin by SPPS using standard Fmoc protocols. Fmoc-Lys(Boc)-OH, Fmoc-Gly-OH, Fmoc-Arg(Pbf)-OH, Fmoc-Gln(Trt)-OH, Fmoc-Gly-OH, Fmoc-Leu-OH, Fmoc-Ala-OH, and Boc-Cys(StBu) were used to assemble the peptides and were purchased from Novabiochem (San Diego, CA). Reactions were carried out in SPPS vessels at room temperature using a stream of dry $N_2$ to provide agitation. Fmoc deprotection was performed by addition of piperidine in DMF (20%, 5 mL) to the Fmoc-peptide resin (0.72 mmol). Deprotection was carried out for 1 × 3 min and 1 × 10 min. Coupling reactions were carried out for 2 h with a mixture of Fmoc-amino acid (2.88 mmol), HBTU (1.06 g, 2.80 mmol), and DIEA (1.25 mL, 7.2 mmol) in DMF. Upon completion of the reaction, the resin was washed with DMF. For TMR-TAT, the Fmoc protecting group at the N-terminus of TAT was cleaved, and the resin was washed with DMF. A mixture of 5,6-tetramethylrhodamine and HBTU (2 and 1.9 equiv in respect to the peptide) in DMF was added to the resin, and the reaction was carried out overnight with gentle shaking. Following chain assembly, the resins were washed with dichloromethane and dried *in vacuo*. The resin was then treated with TFA containing 2.5% $H_2O$ and 2.5% triisopropylsilane for 3 h at room temperature to achieve global deprotection and cleavage from the support. The crude peptide products were precipitated and washed with cold anhydrous $Et_2O$. The precipitates were resuspended in water and lyophilized. The powdery products obtained were then resuspended in 0.1% aqueous TFA/acetonitrile. The peptides were analyzed and purified by reverse-phase HPLC. HPLC analysis was performed on a Hewlett-Packard 1200 series instrument and a Vydac C18 column (5 μm, 4 × 150 mm). The flow rate was 1 mL/min, and detection was at 214 nm. Semipreparative HPLC was performed on a Vydac C18 10 × 250 mm column. The flow rate was 4 mL/min, and detection was at 214 nm. All runs used linear gradients of 0.1% aqueous TFA (solvent A) and 90% acetonitrile, 10% water, and 0.1% TFA (solvent B). All purified and lyophilized peptides were dissolved to 1 mM in DMSO and diluted with PBS to desired concentrations in

further experiments. The correct identity of the peptides was confirmed by MALDI-TOF mass spectrometry (AXIMA-CFR, Shimadzu, Kyoto, Japan). TAT expected mass, 1395.7 Da, observed mass, 1395.5 Da; E3-TAT expected mass, 3834.4 Da, observed mass, 3835.7 Da; E5-TAT expected mass, 3978.5 Da, observed mass, 3978.8 Da; Fl-E5-TAT expected mass, 4609.3 Da, observed mass, 4605.8 Da; E5-TAT-Fl expected mass, 4495.3 Da, observed mass, 4501.5 Da; E5-R9 expected mass:, 4062.6 Da, observed mass, 4065.3 Da; E5(3,7)-TAT expected mass, 3874.4 Da, observed mass, 3877.1 Da; TAT (TMR-GRKKRRQRRRG-$NH_2$) expected mass, 1865.0 Da, observed mass, 1866.1 Da. To obtain the E3 or E5, E3-TAT and E5-TAT were digested with trypsin at a peptide to enzyme ratio of 1:25 for 5 h at 37 °C. This procedure yielded E3 or E5 with a C-terminal arginine residue and with a yield of 97% (the TAT sequence is digested and the sequence of the product is described in Table 1), as demonstrated by HPLC and mass spectrometry. E3 (GLFGAIAGFIENGW-EGLIEGWYGGR) expected mass, 2667.3 Da, observed mass, 2659.2 Da; E5 (GLFEA IAEFI ENGWE GLIEG WYGGR) expected mass, 2813.3 Da, observed mass, 2809.9 Da.

*Hemolysis Assays*. A membrane lysis assay was performed with human erythrocytes purchased from the Gulf Blood Bank (Galveston, TX). Erythrocytes were centrifuged for 5 min at 1500*g*. The erythrocyte pellet obtained was resuspended in PBS, and this procedure was repeated three times to remove the plasma and buffy coat. The erythrocytes (resuspended in PBS to a 50% suspension) were then diluted 20-fold in PBS of different pH values (adjusted with HCl or NaOH, $4.5 < pH < 7.5$). All peptides were diluted with PBS to desired concentrations and added to a 96-well plate. One hundred microliters of the 2.5% RBC suspension was added into each well. One hundred microliters of hemolytic peptides diluted in PBS from a DMSO stock (100 $\mu$M) to a 2× concentration was added to the RBCs to generate a 1.25% suspension of cells with peptides at the desired concentration. To test the effects of heparan sulfate, aliquots of heparin sodium salt (sigma) stock in PBS (100 mg/mL) were used to obtain a final concentration of 1−7 mg/mL. Addition of heparin was done prior to the addition of peptide to the RBC suspension. The plates were incubated at 37 °C for 30 min. After the plate was centrifuged for 5 min at 1500*g*, the supernatants were transferred to a new 96-well plate. The absorbance of hemoglobin present in each well was measured at 450 nm using a plate reader (Bio-Rad; Ultramark Micro plate system). One hundred percent hemolysis was obtained by incubating the RBC with 0.1% Triton X-100. Background hemolysis at various pHs was evaluated by incubating the erythrocytes in the corresponding PBS solutions. The obtained data were plotted using the software KaleidaGraph (Synergy Software, Reading, PA). The data were fitted to an equation of the form $\% = \%\ \min + (\%\ \max - \%\ \min)[H^+]/([H^+] + K50)$, where % max and % min are the maximum and minimum lysis activities observed and K50 is the proton concentration at which $\% = (\%\ \max + \%\ \min)/2$, with $R^2$ between 0.99, 0.97, 0.98, and 0.96 for E3-TAT, E5-TAT, E3, and E5, respectively.

*Giant Unilamellar Vesicles*. The phospholipids 1,2-dipalmitoyl-*sn*-glycero-3-phosphocholine (DPPC), 1,2-dipalmitoyl-*sn*-glycero-3-phospho-L-serine (DPPS), sphingomyelin (brain, porcine) (SM), and cholesterol were purchased in chloroform or chloroform/methanol or as a lyophilized powder from Avanti Lipids. Aliquots were made for each component and the solutions stored in glass vials under nitrogen at −20 °C. Giant unilamellar vesicles (GUVs) were produced by electroformation from Pt wires. The electroformation apparatus was machined using an aluminum block according to the guidelines by Manley and Gordon (*27*). For neutral GUVs DPPC, cholesterol, and SM chloroform solutions were mixed together in a glass vial in a 50:30:20 ratio with a final lipid concentration of 1.0 mM. For anionic GUVs, DPPS was included as 7 mol % of total lipid while maintaining the molar ratio of the other lipid components. Three to four drops of the lipid solutions were applied to each Pt wire using a Hamilton glass syringe, and the apparatus was placed in a vacuum desiccator for at least 1 h to ensure complete solvent removal. The apparatus was then heated at 80 °C, above the highest lipid phase transition temperature in the mixture, and filled with 50 mM HEPES at pH 7 with 150 mM sucrose. An alternating current was applied to the Pt wires by a function generator at 10 Hz and 0.5 V for 2 h, after which the current was stopped and the solution transferred to a glass vial. Peptides were incubated with 20 $\mu$L of this stock GUV solution for 10 min before diluting to a final volume of 200 $\mu$L (1 $\mu$M final peptide concentration) using 150 mM glucose with either 50 mM HEPES at pH 7 or 50 mM acetic acid at pH 4.5. The glucose suspension of GUVs was placed in an eight-well plastic Lab-tek chamber with glass slide bottom and allowed to settle for 15 min before imaging.

*Microscopy Assays*. Hemolytic peptides were added to the 1.25% RBC suspension in PBS at pH of 4.5 or 7 by dilution from their DMSO stock to the desired final concentration (final DMSO content was kept below 5% in all experiments). After incubation at 37 °C for 20 min, 200 $\mu$L of these suspensions was added to the wells of an eight-well chamber glass slide (Nunc). Cells were placed on an inverted epifluorescence microscope (Model IX81; Olympus, Center Valley, PA) equipped with a heating stage maintained at 37 °C. Cells were typically allowed to settle to the bottom of the dish for 5 min prior to imaging so as to obtain a layer of cells in the focal plane. The microscope is configured with a spinning disk unit to perform both confocal and wide-field fluorescence microscopy. Images were collected using a Rolera-MGI Plus back-illuminated EMCCD camera (Qimaging, Surrey, BC, Canada). Images were acquired using bright field imaging and two standard fluorescence filter sets: Texas Red (Ex = 560 ± 40 nm/Em = 630 ± 75 nm) and FITC (Ex = 482 ± 35 nm/Em = 536 ± 40 nm). For time-lapse experiments, the hemolytic peptides, prepared as 2× solutions in PBS at pH 4.5 or 7, were added directly to the 1.25% RBC suspension already placed on the microscope. To wash ghosts, 200 $\mu$L of 2.5% RBC suspension with the hemolytic peptides was centrifuged for 5 min at 1500*g*. The supernatant was removed, and cells were resuspended in 200 $\mu$L of fresh PBS at a desired pH. A 20 $\mu$L aliquot of the cells was added to an eight-well glass slide and imaged to monitor the morphology and fluorescence of cells. These steps were repeated three to five times or until spherical ghosts could not be recovered. An aliquot of 10 kDa FITC-dextran (Invitrogen) was added to the resuspendend ghosts to a final concentration of 250 $\mu$M. The bright field and fluorescence intensities of cells and ghosts were measured using the SlideBook 4.2 software (Olympus, Center Valley, PA). Mean intensities within cells imaged were measured as the total intensity of the cell divided by its area. Annexin V-FITC (ApoDETECT Kit; Invitrogen) was incubated with RBCs lysed with E5-TAT (1 $\mu$M) at pH 6 according to the vendor's recommended protocol (10 $\mu$L of stock solution to 190 $\mu$L of cell suspension in PBS supplemented with 2.5 mM $CaCl_2$).

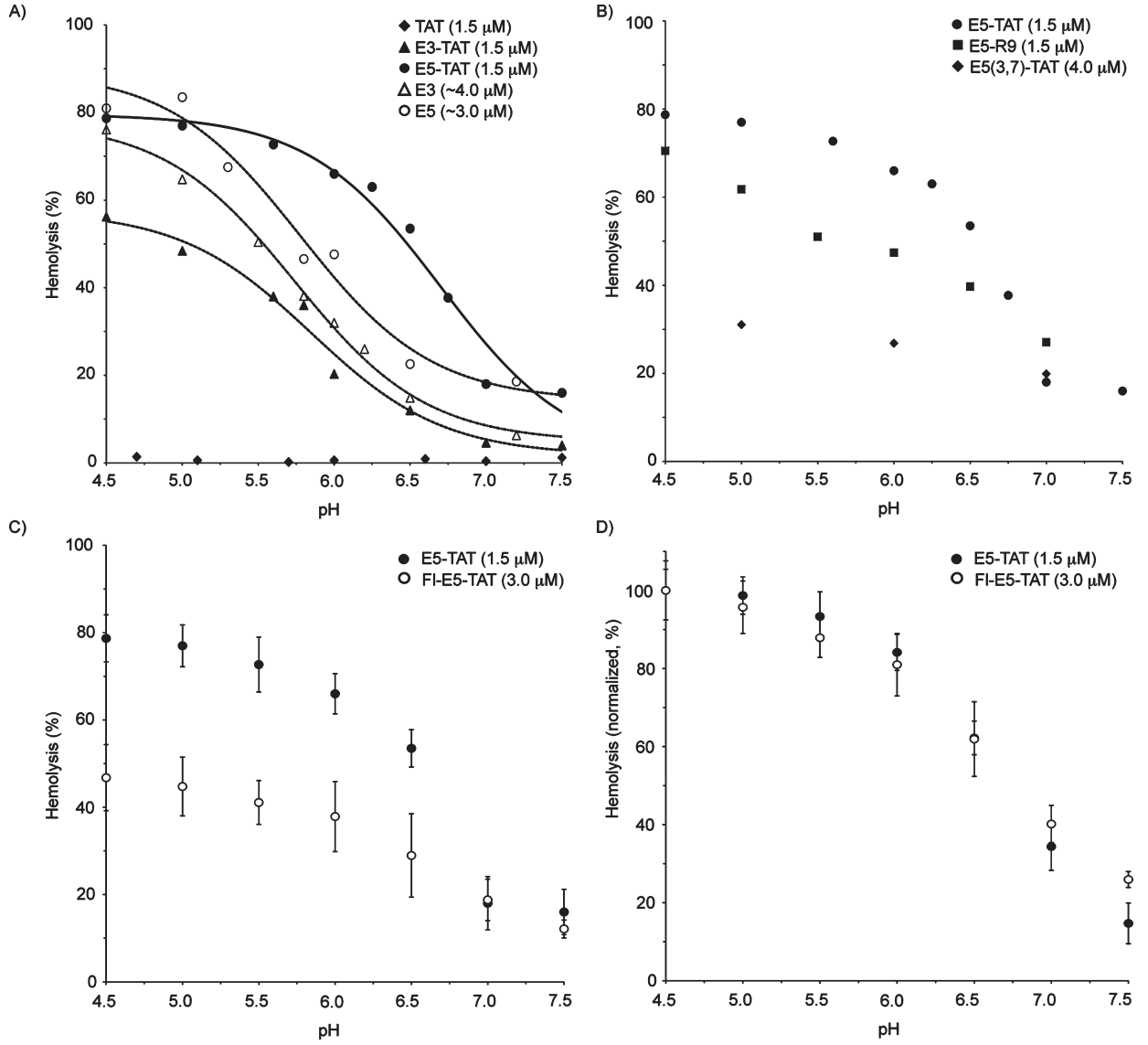


FIGURE 1: (A) Hemolysis activities of HA2 and HA2-TAT analogues as a function of pH. Hemolysis is reported as a percentage of the maximal release of hemoglobin obtained by treatment of the red blood cells with the detergent Triton X. TAT shows no lysis activity while E3, E5, E3-TAT, and E5-TAT display sigmoidal response curves. E3, E5, and E3-TAT have a similar pK50 of approximately 5.7. In contrast, E5-TAT displays a pK50 of 6.7. E3 and E5 are overall less active than E3-TAT or E5-TAT as they require higher concentrations to achieve similar hemolysis percentages at pH 4.5. The plot fitting was performed as described in the Experimental Procedures. The data represent the average of at least three experiments. The standard deviation for each data point, not represented for clarity, was 5% hemolysis or less. Note that the concentration of E3 and E5 reported might be overestimated as the peptides might aggregate and precipitate during the experiment. These data might therefore not accurately reflect the hemolytic activity of the peptide precisely,but, on the other hand, serve to establish the differences in pK50 between the HA2 peptides and their HA2-TAT analogues. (B) Hemolysis results for E5-R9 and E5(3,7)-TAT. (C, D) Comparison of the hemolytic activities of E5-TAT and Fl-E5-TAT. While Fl-E5-TAT has a lower HD50 than E5-TAT, both peptides have an identical pK50.

## RESULTS

*Peptide Design*. Several HA2-TAT analogues were synthesized by solid-phase peptide synthesis (SPPS). Three HA2 analogues were considered in our study: E3, E5 (or E5(4,8)), and E5(3,7) (Table 1). E3 consists of the wild-type HA2 sequence (residues 1−23, strain X31) modified with the mutations M17L and D19E in order to avoid methionine oxidation and aspartyl isomerization during synthesis. E3 contains the residues Trp-21 and Tyr-22 because these residues appear to increase the hemolysis activity of HA2 peptides (*19*). E5 differs from E3 by including the G4E and G8E mutations. Addition of these two glutamate residues has been demonstrated to increase the lysis activity of HA2 analogues (*19*, *26*, *28*). E5(3,7) contains the mutations F3E and A7E described by Wu and co-workers (*29*). TAT was placed at the C-terminus of the HA2 analogues so as not to affect the insertion of the HA2 peptides into membranes (*15*, *30*). In E5-R9, TAT was substituted for R9, a CPP where all of the residues of TAT are mutated to arginine residues (*31*, *32*). For fluorescence labeling, fluorescein isothiocyanate (Fl) was introduced at the N- or C-terminus of E5-TAT during solid-phase assembly to generate Fl-E5-TAT or E5-TAT-Fl, respectively. Fl-E5-TAT was synthesized after E5-TAT-Fl was found to be poorly soluble. Modifications at the N-terminus of HA2 have however been found to reduce the fusion and hemolytic activities of HA2 analogues because it is the N-terminus of HA2 that inserts into lipid bilayers (*15*, *30*). Therefore, in order to minimize the effect that the fluorophore might have on the peptide's activity, the flexible linker 6-aminohexanoic acid (Ahx) was incorporated during synthesis between Fl and the N-terminal glycine. Fl-E5-TAT was found to closely mimic the hemolytic

activity of E5-TAT (Figure 1C,D). Fl-E5-TAT was therefore preferred as the fluorescent analogue of E5-TAT used to visualize the peptide interacting with cellular membranes.

Numerous studies with the HA2 fusion peptide have shown that this amphiphilic peptide behaves poorly in water, making the biochemical study of its properties difficult. Han and Tamm have reported the design of host−guest systems where lysine-rich unstructured C-terminal sequences could solubilize N-terminal HA2 guest sequences (*33*). We therefore reasoned that the highly charged TAT peptide could promote the same effect. The solubility of the peptides E3-TAT and E5-TAT in aqueous buffers was first assessed by monitoring the extent to which the peptides remain in solution for extended periods of time. The peptides were dissolved in PBS to 5 $\mu$M, and the samples were centrifuged at high speed every hour to separate the soluble peptides from possible precipitate. The concentration of the peptides remaining in solution was then determined by HPLC analysis. Under these conditions, all peptides appeared to remain in solution for at least 24 h (data not shown). To determine the effect that TAT might have on the solubility of the amphiphilic HA2 sequences, the control peptides TAT, E3, and E5 were also synthesized by SPPS. TAT was obtained in high yield, but this approach did not yield satisfactory results for E3 and E5 as the peptides precipitated and degraded after HPLC purification and storage (data not shown) (*34*). Instead, E3 and E5 were obtained by trypsin-mediated cleavage of the TAT peptide from E3-TAT and E5-TAT. HPLC and mass spectrometry analysis confirmed that single E3 or E5 products with a C-terminal arginine were produced with less than 3% of the uncleaved peptide remaining. Using this approach, the peptide was found to be soluble and stable in PBS for at least 1 h at room temperature. However, like the synthesized peptides, the E3 and E5 peptides produced by TAT cleavage also showed a tendency to precipitate and degrade over time as determined by HPLC and mass spectrometry analysis (we were however unable to determine the nature of the degradation products because of their low solubility; data not shown). Overall, these results suggest that the highly charged and hydrophilic TAT sequence has a solubilizing and stabilizing effect on the amphiphilic E3 and E5 sequences.

*HA2-TAT Peptides Lyse Erythrocytes in a pH-Dependent Manner*. The pH-dependent hemolysis activities of the HA2-TAT peptides were characterized by an *in vitro* erythrocyte lysis assay. The peptides were incubated with human RBCs in PBS with the pH adjusted to different values. The release of hemoglobin from lysed cells was then measured spectrophotometrically at 450 nm 30 min after incubation was initiated (hemolysis is complete at this time point in all of our assays). E3-TAT, E5-TAT, E3, and E5 all show a clear pH-dependent lysis activity and display sigmoidal response curves consistent with a single protonation model (Figure 1A). E3-TAT, E3, and E5 displayed an identical apparent pK50 of approximately 5.8 (pH at which 50% of maximum hemolysis is obtained). This pK50 is consistent with values reported for HA2 peptides and the X-31 virus itself (*15*, *35*). In contrast, the hemolysis response curve of E5-TAT is significantly shifted toward higher pH and displays an apparent pK50 of 6.7. E5-TAT also appears to have a higher activity than E3-TAT at all pHs (Figure 1A). The activities of E3 and E5 were much reduced in comparison to E3-TAT and E5-TAT. E3 and E5 required a concentration of approximately 4 or 3 $\mu$M to display a hemolysis activity at pH 4.5 similar to that of E3-TAT and E5-TAT at 1.5 $\mu$M. A precise comparison of the activity of the E3/5-TAT and E3/5 peptides was however rendered difficult because of the poor solubility of E3/5. Finally, TAT did not induce erythrocyte lysis at any of the concentrations (up to 80 $\mu$M) or pH values (4.5−7.5) tested. Together, these results indicate that the increase in activity and the change in pH response observed for E5-TAT appear to be dependent on the presence of both TAT and the G4E and G8E mutations since neither E5 nor E3-TAT displays the same characteristics.

The origin of the unique behavior of E5-TAT was further investigated with E5(3,7)-TAT and E5-R9 (Figure 1B). E5(3,7)-TAT was used to evaluate the effect of the position of the Glu residues in the HA2 peptide. E5-R9 was used to determine whether the observed effects were only due to the arginine-rich nature of TAT. TAT was therefore replaced with another positively charged peptide, R9. E5(3,7)-TAT activity was much reduced in comparison to E5-TAT. Interestingly, Wu and coworkers have shown that the pKa values for the glutamate residues Glu3 and Glu7 of E5(3,7) in SDS micelles were elevated by more than a pH unit in comparison to Glu4 and Glu 8 of E5(4,8) (*29*). We observe however that the overall pK50 of E5(3,7)-TAT was reduced in comparison to that of E5-TAT. The hemolysis response curve of E5-R9 was not sigmoidal. This highlights the fact that the behavior of this peptide was quite different from that of E5-TAT and that the composition and sequence of TAT play a role in the pK50 shift observed for E5-TAT.

The effect of the concentration of peptide used during the hemolysis was evaluated for E5-TAT and Fl-E5-TAT. The results obtained with the fluorescently labeled peptide are shown in Figure 2A. The HD50 (hemolytic dose for 50% lysis) of E5-TAT and Fl-E5-TAT were approximately 2.6 and 10.2 $\mu$M at pH 7.0, respectively, and 0.5 and 1.8 $\mu$M at pH 4.0, respectively (note that these values are dependent on the number of RBCs present in suspension; see Supporting Information Figure S1). In both cases, the hemolytic activity of the peptide is increased approximately 5-fold when the pH is decreased from 7.0 to 4.0. Despite an overall decrease in the activity of Fl-E5-TAT as compared to E5-TAT, the pK50 of both peptides were identical at 6.7 (Figure 1D). Overall, these data suggest that Fl-E5-TAT is a fluorescent analogue of E5-TAT that can closely reproduce its properties.

*E5-TAT Binding to Red Blood Cells Is pH-Dependent*. The hemolytic activity and binding of Fl-E5-TAT to RBCs were investigated by microscopy. The lysis of RBCs after peptide addition was detected by the decrease in the cells' optical contrast observed by bright field microscopy and as reported by Jay and Rowlands (*36*). The products of the lysis were ghost cells with a visible membrane but with an interior invisible upon bright field imaging (Figure 2B). This is consistent with cells losing their content as lysis proceeds and with the lumen of the ghost being filled with the surrounding media. Lysis was also confirmed by monitoring the loss of red autofluorescence of RBCs upon ghost formation (Figure 2B). It is important to note that the red fluorescence present inside the RBCs cannot be accounted by hemoglobin as hemoglobin has been clearly shown to be poorly fluorescent. Instead, porphyrins and other metabolites are more likely to be the fluorescent material observed in these experiments (*37*). Yet, loss of autofluorescence further confirms that the lysed RBCs are losing their content. In our hands, loss in optical contrast in bright field imaging and loss of red autofluorescence were simultaneous (data not shown).

Red blood cells were incubated with Fl-E5-TAT at pH 4.5 or 7.0, and the binding of the peptide to membranes was monitored

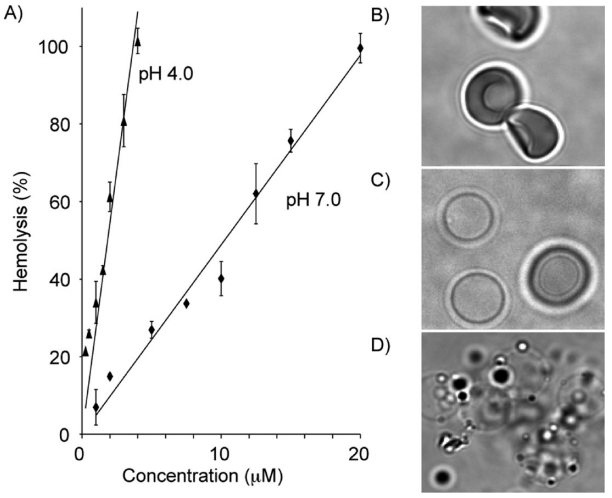


FIGURE 2: (A) Hemolytic activities of Fl-E5-TAT at pH 7.0 (diamonds) and 4.0 (triangles) as a function of peptide concentration and for 1.25% RBC suspensions. The data fit the equations $y = 27.2x$ at pH 7 and $y = 4.9x$ at pH 4.0 with $R^2$ of 0.90 and 0.98, respectively. The HD50 of the peptide are 1.8 and 10.2 $\mu$M at pH 4.0 and 7.0, respectively. (B) Bright field image of intact RBCs in the absence of peptide. (C) Bright field image of ghosts obtained by E5-TAT-mediated hemolysis of RBCs at pH 4.5 and at a concentration below the HD50 of the peptide at this pH. (D) Bright field image of RBCs lysed by E5-TAT at pH 7.0 at a concentration twice its HD50. Ghosts fuse to one another and their membranes collapse rapidly after addition of the peptide.

by fluorescence microscopy (Figure 3). Fl-E5-TAT was first incubated with RBCs at pH 7.0 and at a concentration below its HD50 (5 $\mu$M, HD50 = 10.2 $\mu$M) so as to prevent extensive lysis. The fluorescence of Fl-E5-TAT appeared to be diffused in solution, and no association of the peptide to the membrane of RBCs could be observed. In contrast, when incubated at pH 6.0, 5.0, or 4.5, the peptide was found to increasingly accumulate at the surface of intact RBCs (Figure 3 and Supporting Information Figure S2; a concentration of 1 $\mu$M peptide was used to minimize lysis). Together, these results suggest that Fl-E5-TAT remains predominantly soluble at pH 7.0 but associates with the membrane as the pH decreases.

Addition of the E5-TATor Fl-E5-TAT to RBCs incubated at pH 4.5 at concentrations above their HD50 (5 $\mu$M) induced rapid lysis. Prior to lysis, RBCs appeared as a mixed population of concave and spherical cells. The presence of spherical cells is consistent with the swelling observed when concave cells are exposed to stress such as low pH (*38*). Lysis of cells that were initially spherical did not appear to induce an observable change in the diameter or morphology of the cell (Figure 2B). Initiation of lysis after E5-TAT addition was different from cell to cell, but once initiated, lysis was complete in 90 ± 30 s on average to reach completion (average and standard deviation obtained from a population of 50 cells) (Figure 4). Similar results were obtained for E5-TAT and Fl-E5-TAT. In the case of Fl-E5-TAT however, binding of the fluorescent peptide to the surface of ghosts was clearly observable by fluorescence microscopy (Figure 3). RBCs that were not lysed by the end of the experiments typically showed little fluorescence and peptide binding on their surface.

*Fl-E5-TAT Permeabilizes Membranes in a Manner Not Reversed by Dilution or pH*. Next, we tested whether the ghost obtained by E5-TAT-mediated hemolysis remained permeable after hemolysis and whether permeability could be reversed. Ghosts were obtained by treatment of RBCs with E5-TAT at pH 4.5. The ghosts were then either kept in the pH 4.5 media with

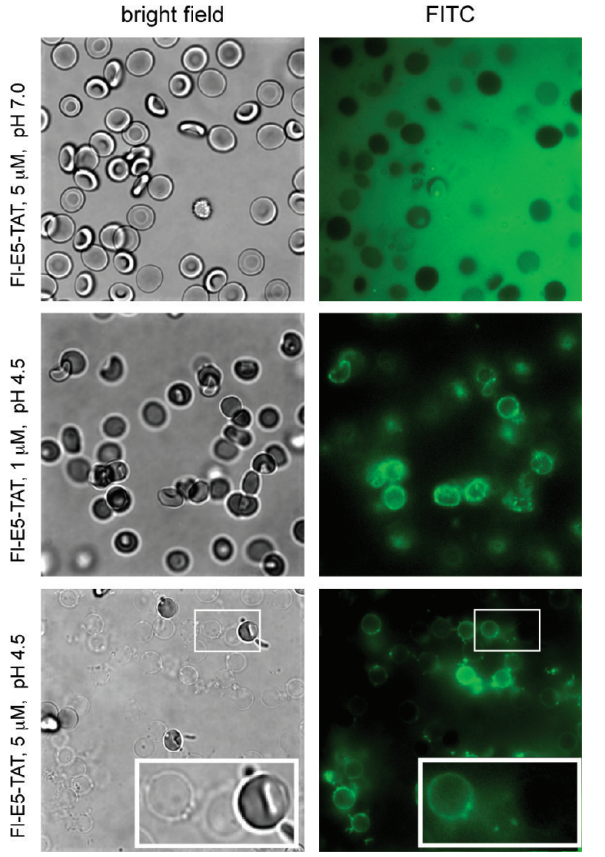


FIGURE 3: Binding of Fl-E5-TAT to RBCs and ghosts as a function of pH. RBCs were incubated with 1 or 5 $\mu$M Fl-E5-TAT at pH 7.0 or 4.5, and the samples were observed by fluorescence (Fl-E5-TAT, FITC image, pseudocolored green) and bright field (RBCs/ghosts) microscopy. At pH 7.0 and at a low concentration of peptide (5 $\mu$M, below the HD50 at pH 7.0), the RBCs are intact, and the peptide appears to be homogeneously distributed in solution. No binding to the surface of the RBCs is detected under these conditions. At pH 4.5 and at 1 $\mu$M peptide (below the HD50 at this pH), the RBCs remain intact, but the peptide appears to preferentially partition at the membrane of the cells. At pH 4.5 and 5 $\mu$M peptide (above the HD50 at this pH), the RBCs are lysed, and the peptide binds to the membrane of the ghosts formed.

the E5-TAT peptide present or washed with fresh pH 4.5 or 7 PBS buffer at 37 °C. These latter steps consisted of a repeated dilution protocol as ghosts could not be washed under stringent conditions without loss of membrane integrity and membrane collapse. A 10 kDa dextran-fluorescein was then added to the RBCs and ghosts, and the samples were then observed by fluorescence microscopy. Intact RBCs had internal fluorescence signals much lower than the fluorescence of the surrounding solution (Figure 5). This is consistent with the dextran not being able to penetrate RBCs. In contrast, ghosts showed an internal fluorescence equal to that of the media. This indicates that the 10 kDa dextran-fluorescein had freely penetrated into the ghosts and that the ghosts remained permeable to macromolecules (Figure 5). Fluorescence imaging was also performed immediately after diluting the media of the sample. As seen in Figure 5, fluorescent ghosts were clearly observed over a darker background, further confirming that the fluorescent dextran had penetrated the ghost. Similar experiments were reproduced with Fl-E5-TAT. This time, fluorescence imaging revealed that the Fl-E5-TAT peptide was still bound to the membrane even after repeated dilutions and washing steps at either pH 4.5 or pH 7 (Figure 5). Together, these results suggest that the peptide

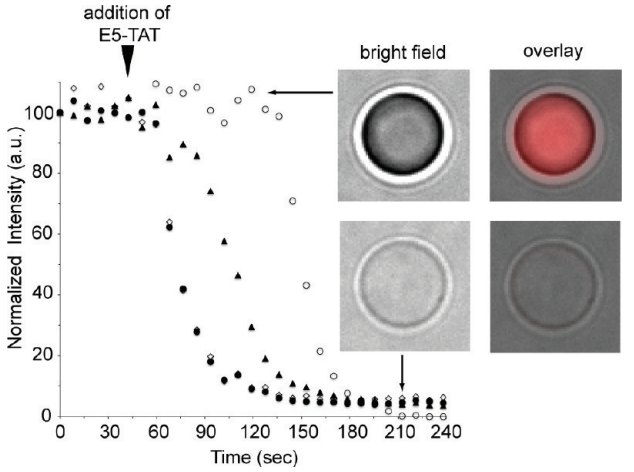


FIGURE 4: Time course of lysis and ghost formation from single red blood cells determined by fluorescence and bright field microscopy. RBCs were incubated in PBS at pH 4.5 and imaged every 10 s in a time-lapse experiment. After 50 s, the cells were treated with 1 $\mu$M E5-TAT, and imaging was immediately resumed. Lysis was assessed by measuring the decrease in optical contrast of cells in the bright field image (data displayed) or the decrease in their autofluorescence in the red fluorescence image (not represented but identical results were obtained using this method). Cell leakage appears to be initiated at slightly different times. Once initiated, lysis consistently took on average $90 \pm 30$ s to reach completion ($n = 50$ cells, four represented in the figure). Bright field and fluorescence overlay images (cell autofluorescence, pseudocolored red) show that the morphology of the cells does not change during the experiment and that their diameter remains approximately constant.

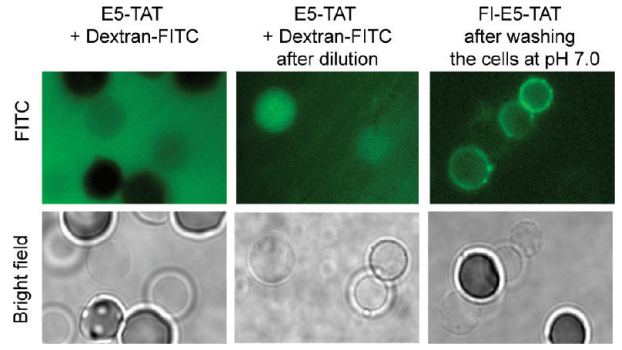


FIGURE 5: Ghosts remain permeable after lysis, and Fl-E5-TAT remains tightly bound to their membranes. The fluorescent marker 10 kDa dextran-FITC was added to cells lysed by treatment with E5-TAT (3 $\mu$M) at pH 4.5. A clear fluorescence contrast is observed between the exterior and interior of intact RBCs. Conversely, ghosts display a fluorescence signal similar to that of the media surrounding them, suggesting that the fluorescent dextran is able to penetrate ghosts but not intact RBCs. Rapid dilution of the media generates a higher fluorescence contrast inside ghosts, confirming that the dextran is present in the lumen of ghosts. Binding of Fl-E5-TAT to ghosts is maintained after washing at pH 7. Ghosts were formed by treating RBCs with 3 $\mu$M Fl-E5-TAT at pH 4.5. The ghosts were then washed with PBS at pH 7.0 and imaged by fluorescence microscopy. Staining of the ghosts by the peptide was not reduced by repeating the washes or with time. Similar results were obtained when the pH of the PBS was 4.5 (data not shown).

remains stably anchored to the ghost membrane at either low or neutral pH and that this results in the formation of ghosts that are not resealed.

*Peptide Binding to Red Blood Cells and GUVs Is Dependent on Membrane Composition*. During the course of our experiments, we observed that the fluorescence at the membrane of ghosts increased during lysis and occasionally after lysis had taken place. This suggested that binding of the peptide might not be dependent on pH only but on changes in membrane composition that might occur during lysis. To address this issue, we first tested whether the TAT sequence might be involved in this effect. TAT labeled with fluorescein, Fl-TAT, was added to RBCs at either pH 4 or pH 7. In both cases, no staining of the RBCs' membranes and no lysis could be observed. However, addition of Triton X and lysis led to an immediate increase in membrane staining at both pHs (Figure 6). Binding of Fl-TAT to the membrane of the ghosts formed by treatment with E5-TAT at pH 4.5 could also be observed. However, the contrast between the signal in solution and the signal at the membrane was much reduced in this experiment, suggesting that E5-TAT and TAT are competing for binding. Together, this indicates that TAT binds to lysed cells and that TAT has access only after lysis to membrane components that are not accessible before lysis. In particular, we reasoned that these observations could be the result of the binding of TAT to negatively charged phospholipids. Interestingly, phospholipid phosphatidylserine (PS) is known to be predominantly present at the inner leaflet of the membranes of intact erythrocytes (*25*, *39*). TAT has also been reported to bind liposomes containing anionic phospholipids (*24*, *40*). TAT and E5-TAT could therefore bind to PS after E5-TAT-mediated hemolysis. PS could for instance flop through the aqueous pores formed during lysis and become exposed on the surface of the cells. Alternatively, E5-TAT could have access to luminal PS after lysis and diffusion into the permeable ghost. In order to test whether PS might be involved in the observed E5-TAT and TAT binding to ghost cells, FITC-annexin V, a fluorescently labeled protein with an extremely high affinity for PS, was added to ghosts obtained by E5-TAT-mediated hemolysis (*41*). As shown in Figure 6B, labeling of the membrane of ghosts by annexin V could be clearly observed while no labeling was observed for intact RBCs. To further determine whether PS might contribute to TAT binding to the membrane of ghosts, the affinity of this peptide for PS was assessed by monitoring the binding of the peptide with giant unilamellar vesicles (GUVs). GUVs containing the neutral lipids 1,2-dipalmitoyl-*sn*-glycero-3-phosphocholine (DPPC), choline sphingomyelin from stearic acid (SM), and cholesterol were prepared as models for the outer leaflet of erythrocyte. GUVs containing the negatively charged 1,2-dipalmitoyl-*sn*-glycero-3-phospho-L-serine (DPPS) (9 mol %) in addition to the neutral lipids were prepared as models for the inner leaflet of erythrocytes. TAT, labeled with the fluorophore 5(6)-carboxytetramethylrhodamine (TMR), was incubated with the GUVs at pH 4.5 or 7, and the distribution of the peptide was assessed by fluorescence confocal microscopy (Figure 6). TMR-TAT was diffusely distributed in the media at either pH 4.5 or pH 7 when incubated with GUVs lacking DPPS. No apparent accumulation of the peptide at the membrane of the GUVs could be detected. In contrast, TMR-TAT fluorescence strongly stained the membrane of GUVs containing DPPS. This behavior was observed at either pH 4.5 or pH 7, indicating that pH does not influence binding under these conditions. Together, these results suggest that the presence of negatively charged lipids such as PS can dramatically increase the affinity of TAT for membranes.

*Heparin Inhibits Membrane Binding of E5-TAT and Hemolysis*. Other negatively charged molecules that TAT might interact with are the glycosaminoglycans present on the surface of mammalian cells. In particular, TAT binds to cell-surface heparan sulfate (HS) proteoglycans, and this interaction appears

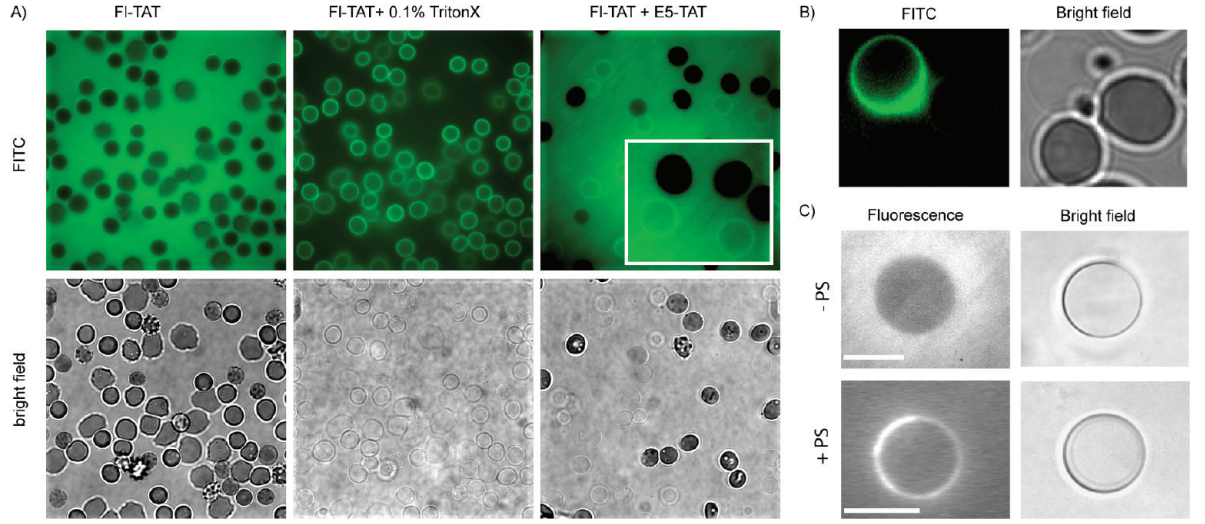


FIGURE 6: (A) Binding of Fl-TAT to RBCs and ghosts. Fl-TAT (5 $\mu$M) was added to 1% RBCs, and the cells were observed by phase contrast and fluorescence microscopy. Fl-TAT appears to be diffusely distributed in solution and no accumulation of the peptide on the membrane of RBCs can be detected under these conditions. Addition of 0.1% Triton X results in rapid lysis of the RBCs. Fl-TAT is then observed to bind to the membrane of the formed ghosts. The set of images after addition of Triton X represents the same field of cells represented before addition and was acquired less than 10 s after addition of the detergent. Fl-TAT also binds to ghost obtained by E5-TAT-mediated hemolysis. RBCs were treated with 1 $\mu$M E5-TAT at pH 4.5, and Fl-TAT (5 $\mu$M) was added to the sample. While binding of Fl-TAT to the membrane of ghosts is clearly visible, the fraction of peptide that remains in solution appears much larger than in the Triton X experiment. The data represented were obtained at pH 4.5, but similar results were obtained at pH 7 (data not shown). (B) Annexin V binds to ghosts but not to intact RBCs. Cells were exposed to 1 $\mu$M E5-TAT at pH 6 to generate a mixture of intact RBCs and ghosts. The sample was treated with FITC-annexin V, and binding of annexin V to membranes was detected by fluorescence microscopy (FITC image, pseudocolored green). (C) Binding of TMR-TAT to GUVs. The fluorescent peptide binds to GUVs containing DPPS (+PS, GUV membrane staining) but not to GUVs lacking it (−PS, diffuse fluorescence in media). The scale bars represent 10 $\mu$m.

to play a key role in the translocation of the peptide inside cells. Degradation fragments of HS are present within endocytic compartments, and these molecules have been proposed to inhibit the interaction of TAT with endosomal lipid bilayers and thereby reduce the efficiency with which the peptide can escape from endosomes (see Discussion). We were therefore interested in determining whether binding of E5-TAT to HS degradation fragments would inhibit the lytic activity of the peptide. To test this hypothesis, RBCs incubated with the HS analogue heparin were used to model the lumen of endosomes that would contain soluble HS degradation fragments. E5-TAT was added to samples of heparin/RBCs, and the extent of hemolysis was measured spectrophotometrically. E5-TAT-mediated hemolysis at pH 4.5 was greatly reduced when RBCs were incubated with heparin (Figure 7A). The extent of this inhibition was dependent on the concentration of heparin used, and hemolysis could be almost completely abolished when a large excess of heparin was used (10 mg/mL; data not shown). On the other hand, the hemolysis activity of E5 was not affected by addition of heparin at any of the concentrations tested (1−10 mg/mL). In addition, binding of Fl-E5-TAT to the surface of RBCs at pH 4.5 was greatly reduced when heparin was added to the media (Figure 7B). Together, these results suggest that heparin inhibits the binding of the peptide to the membrane of RBCs. As a consequence, the peptide is then unable to cause hemolysis.

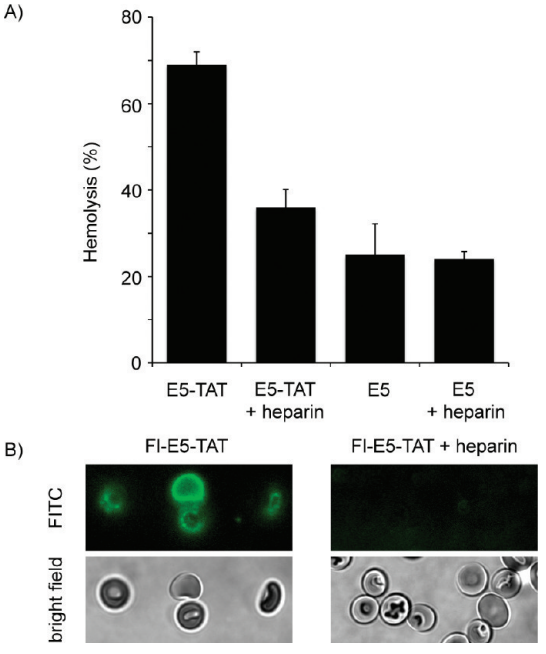


FIGURE 7: (A) Heparin inhibits the hemolytic activity of E5-TAT but not that of E5. RBCs were treated with 3 $\mu$M E5-TAT or E5 at pH 4.5 in the absence or presence of heparin (1 mg/mL). (B) Heparin inhibits the binding of Fl-E5-TAT to the membrane of RBCs. RBCs were treated with 1 $\mu$M Fl-E5-TAT at pH 4.5 in the absence or presence of heparin (1 mg/mL). No binding of the peptide to the membrane is observable when heparin is present in the sample and hemolysis is inhibited (RBCs in the image are intact).

## DISCUSSION

The delivery peptides investigated in this study are chimeric peptides derived from the HA2 fusion peptide of influenza hemagglutinin protein and the TAT peptide derived from the HIV transactivator of transcription protein (residues 47−60). These HA2-TAT peptides are designed to combine the endocytosis-inducing activity of TAT and the pH-dependent endosomal release activity of HA2. Our results however highlight a complex interplay between the two peptides and several important parameters that affect their lytic activities. The first evidence of how TAT might affect the activity of HA2 peptides is given by the

increase in hemolysis activity measured between E3/E5-TAT and E3/E5. It is well established that HA2 peptides are poorly soluble. Addition of the hydrophilic TAT sequence could therefore reduce the aggregation propensity of the HA2 peptides and be the cause of the increase in activity observed (*42*). Tamm and co-workers have indeed reported that addition of lysine residues to the C-terminus of HA2 sequences could greatly increase the solubility of the peptides (*33*). Consistent with this idea is our observation that E3 or E5 would rapidly aggregate and degrade during our experiments while E3/E5-TAT would not. The effect of TAT on the activity of E5 was however more pronounced than on the activity of E3. In particular, a dramatic shift in the hemolysis pK50 could be observed, and this effect appeared dependent on the presence of both TAT and the G4E and G8E mutations. This suggests the presence of electrostatic interactions between the positively charged residues of TAT and the glutamate residues of E5. Tsien and co-workers have indeed reported that the addition of polyglutamate sequences to arginine-rich cell-penetrating peptides results in intramolecular electrostatic interactions that block the cell-penetrating activity of the peptides (*43*). We have reported that E5-TAT, despite containing TAT, binds to a lesser extent than TAT to a negatively charged protein such as BSA (*21*). This suggests that the TAT sequence in E5-TAT has a reduced affinity for negatively charged molecules because it might be involved in intramolecular interactions with E5. Yet, one would expect that these interactions would stabilize E5 in its deprotonated form and lead to a decrease in the pKas of the glutamate residues and in hemolysis pK50. This is however contrary to our observations. Another possibility to explain for the observed increase in pK50 then might be that TAT increases the affinity of E5 for the lipid bilayer. HA2 peptides form amphipathic helices in membrane environments and upon protonation of their glutamate residues (*44*, *45*). The helices adopt a boomerang or hairpin-shaped structure at the lipid/water interface with hydrophobic residues facing the lipid environment. Based on these structures, the five Glu residues of E5 are expected to be located in close proximity on the interface exposed to water. Binding of E5-TAT to the membrane could therefore promote helix formation, leading to a clustering of the glutamate residues and to unfavorable like-charge repulsion between these residues. This would in turn facilitate the protonation of the Glu residues to avoid unfavorable Coulombic interactions and lead to an elevation of their pKa and of the pK50 observed (*46*). These effects would be diminished or absent in E3-TAT or E5(3,7)-TAT because E3 has fewer Glu residues than E5 and because the Glu residues of E5(3,7) are further away from one another when one considers their distribution on a helical wheel.

To understand how E5-TAT disrupts membranes, the mechanism by which hemolysis is achieved was further explored. Like other HA2 peptides described, E5-TAT and Fl-E5-TAT exist in equilibrium between soluble and membrane-bound states (*47*). As observed by microscopy, a decrease in pH, and presumably protonation of the peptide glutamate residues, shifts this equilibrium to the membrane-bound state as the solubility of the peptide is reduced. Similar pH-dependent membrane partitioning has been observed for AcE4K, an HA2 analogue similar to the E5 and Fl-E5 sequences used in this study (*47*). Our hemolysis data are consistent with a single protonation model where the peptides undergo a transition from a soluble and nonlytic state $A^-$ to a membrane-bound and lytic state HA. The pK50 obtained from the hemolysis plot can then be interpreted as an acid dissociation constant for the $A^-$/HA pair. In addition, the HD50 obtained at pH 4 and 7 represent the same total concentration of HA if one considers the Henderson−Hasselbach equation of the form $pH = pK50 + \log [A^-]/[HA]$. Lysis would therefore appear to only depend on the total amount of HA present in the membrane of RBCs. It is however important to note that the HD50 values correspond to peptide concentrations at which 50% of the RBCs are totally lysed and 50% are intact as opposed to 100% of cells 50% lysed. It therefore appears that the amount of peptide bound to the membrane of single cells has to reach a certain threshold before lysis can be initiated.

When lysis was carried out at concentrations well above the HD50 of the E5-TAT and Fl-E5-TAT, the membrane of ghosts collapsed and fused to one another. In contrast, lysis at concentrations at or below the determined HD50 did not appear to dramatically change the morphology of the membrane, and the diameter of ghosts remained approximately constant under these conditions. Leakage from single cells incubated with E5-TAT was initiated at different times, reflecting the fact that cells are heterogeneous and might have varying degrees of membrane fragilities. Once initiated, lysis was slow since 90 s was required on average to achieve complete hemolysis. Together, these results do not support the formation of dramatic lesions in the membrane as sometimes observed with the hypotonic lysis of RBCs (*48*). Instead, they suggest that cell permeability is induced by the formation of aqueous pores large enough for the passage of hemoglobin or dextrans. The relatively slow leakage observed is also indicative of formation of a limited number of pores with a relatively small diameter rather than very large holes. Indeed, hemolysis by osmotic shock in hypotonic media was observed to be complete in 4 s for single RBCs (*38*, *49*). Considering that the diffusion constant of hemoglobin is approximately $7 \times 10^{-7}$ cm$^2$/s, it was then estimated that hemolysis could be achieved at the observed rate if cells contained 100 pores of a diameter of 70 Å (tetrameric hemoglobin has a spheroidal shape 65 × 55 × 50 Å) (*49*). While such estimates are more qualitative than quantitative since the diameter of pores cannot be accurately determined, similar calculations would indicate that E5-TAT mediates the formation of less than three equivalent pores per cell.

Ghosts obtained by hypotonic osmotic shock typically reseal within seconds in isotonic media and at 37 °C (*49*). In contrast, the ghosts obtained by Fl-E5-TAT-mediated lysis remained permeable to dextrans under similar conditions. Interestingly, Fl-E5-TAT could not be washed from the membrane at either pH 4 or pH 7. This is very different from what has been observed with AcE4K (*47*). A possible explanation for this observation is that TAT might play a role in the stable peptide binding to the membrane. Indeed, our data suggest that, while binding of E5-TAT to intact RBCs or liposomes is dependent on the E5 moiety, the binding of the peptide to ghosts is in part due to the affinity of TAT for the lysed membrane. Fl-TAT did not show significant binding to intact RBCs but was bound to the membrane of ghosts lysed with the detergent Triton X or with E5-TAT. One possible explanation for these observations is that, upon lysis, the peptide is able to access molecules that are not available for binding in intact cells. A possible binding partner is PS, a negatively charged phospholipid which is located on the inner leaflet of the membrane of RBCs (*39*). Our data do not rule out that the peptide binds to other molecules than PS upon lysis but demonstrate that binding to anionic phospholipids such as PS could account for the effects observed. For instance, the affinity of TAT for liposomes containing PS was clearly greater than to that of liposomes lacking this lipid. Futhermore, annexin V, a protein

with a specific affinity for PS, could bind to ghosts obtained by E5-TAT-mediated lysis but not to intact RBCs, suggesting that PS is exposed upon lysis (*41*). We envision two possible mechanisms by which TAT might gain access to PS. First, TAT could bind to PS by diffusing into the ghost and binding to the inner leaflet of the membrane. Alternatively, PS might flop to the outer leaflet of the membrane by diffusing laterally through the aqueous pores that are formed during lysis. The phospholipid asymmetry present in intact cells would therefore be lost upon lysis, and TAT might bind to PS exposed outside the cell. While not mutually exclusive, these two models could not be distinguished because the ghost permeability could not be reversed. It is therefore not possible to prevent the access of molecules into the ghosts and explore whether PS is exposed on the outer or inner membrane leaflets or both.

Overall, the binding of TAT to the lysed membrane of ghosts might contribute to the stable association of the peptide E5-TAT to the lipid bilayer and might explain in part why the peptide could not be washed away and why the permeability could not be reversed. In addition, it raises the possibility that TAT might play an active role in the lysis event. The E5 moiety in E5-TAT is clearly required to trigger lysis since TAT does not cause hemolysis on its own. E5 might be sufficient to initiate the formation of aqueous pores, and TAT might not contribute to this process at first. PS might then diffuse laterally through these pores as outer and inner leaflets are now connected to one another. One can therefore envision how the exposed PS would then lead to more peptide being recruited to this area because of the strong interaction between TAT and PS. This in turn might lead to more membrane disruption and could contribute to the increased activity and pK50 shift observed for E5-TAT when compared to E5.

HA2-TAT analogues can deliver macromolecules into the cytosolic space of mammalian cells. In particular, E5-TAT can cause the release of macromolecules trapped inside endocytic organelles, and this activity is dependent on the acidification of these organelles (*21*). However, the delivery efficiency associated with this peptide remains modest. Improving the properties of this delivery agent requires that one understand how this peptide functions. Yet, it is difficult to characterize the lytic activity of E5-TAT inside endocytic organelles because they represent a chemically complex and dynamic environment. After internalization at the plasma membrane, endocytic vesicles loaded with E5-TAT might undergo multiple steps of maturation, and the peptide might partition into various endocytic organelles, including early endosomes, recycling endosomes, late endosomes, and lysosomes (*50*). These organelles have membranes of different lipid, carbohydrate, and protein composition, and their lumen is acidified to different extents (*50*). We propose however that our results with RBCs might provide valuable insights into how E5-TAT might behave inside endocytic organelles.

Endocytic organelles have a pH ranging from approximately 6.5 for early endosomes to 5.5 in late endosomes and 4.5 for lysosomes (*51*, *52*). The high pK50 observed for E5-TAT would suggest that an increase in the lytic activity of the peptide might occur early in the endocytic pathway. E5-TAT might rapidly bind to the membrane of endosomes as the vacuolar ATPase acidifies the lumen of endocytic organelles and form aqueous pores from which internalized macromolecules could escape (*14*). In contrast, E3-TAT, with its lower pK50, would be activated later in the endocytic pathway. Our data however suggest that parameters other than pH will influence the activity of the peptides, including the presence of heparan sulfate (HS) proteoglycans and the lipid composition of the membrane.

It is now well established that TAT binds to heparan sulfate proteoglycans (HSPGs) on the cell surface and that internalization of TAT is typically reduced in glycosaminoglycan-deficient cell lines (*9*, *53*−*55*). Soluble acidic polysaccharides like heparin can also compete with HSPGs for TAT binding and inhibit the translocation of the peptide into cells (*56*−*58*). The importance of HSPGs for TAT-mediated translocation remains however unclear as TAT might be internalized inside cells by multiple nonexclusive mechanisms that may or may not involve HSPGs (*59*−*61*). While association of TAT to HSPGs might contribute to an increase in peptide uptake, it is also possible that HSPGs may sequester TAT away from the lipid bilayer and reduce its ability to translocate across the plasma membrane (*6*, *62*, *63*). It is also known that TAT induces the internalization of cell-surface HSPGs (*64*). TAT and HSPGs might therefore associate within endocytic compartments, and it is possible that this association inhibits TAT-mediated endosomal release (*62*, *65*). In addition, HS proteoglycans are degraded within the endocytic pathway by sequential endoglycolysis and proteolysis (*66*−*69*). The polysaccharide chains appear to be degraded in a stepwise manner with a progressive reduction in the size of the degradation fragments that correlates with the maturation of the endocytic compartments from early endosomes to lysosomes. Release of HS chains from the HSPG protein moiety and partial cleavage of the soluble HS chains are initiated early on in the endocytic pathway. Degradation of HS fragments one-half to one-fourth the size of the original HS chain does not appear however to be completed until accumulation into lysosomes occurs. It is therefore possible that HS degradation does not precede TAT degradation and that soluble HS degradation fragments inhibit the binding of TAT to lipid bilayers throughout the endocytic pathway. We were therefore interested in testing whether similar effects would be observed for E5-TAT. In particular, binding of TAT to soluble HS might prevent E5 from binding to the phospholipid bilayer. On the other hand, the affinity of E5 for the lipid bilayer might promote the binding of E5-TAT to the bilayer regardless of whether TAT is bound to HS or not. To test the effect that TAT binding to HS might have on E5-TAT activity, the soluble HS analogue heparin was used. RBCs were again used as a model because the surface of RBCs has been shown to contain very low levels of HS proteoglycans (*70*, *71*). RBCs might therefore be comparable to the membrane of endocytic organelles once cleavage of the HS chains from the HSPGs has taken place. In our experiments, the presence of heparin had a dramatic inhibitory effect on the hemolytic activity of E5-TAT but not of E5. The binding of Fl-E5-TAT to RBCs was also much reduced when heparin was present in solution. Together, these results suggest that binding of TAT to heparin sequesters the E5 moiety away from the membrane of RBCs. By analogy, TAT binding to HS or HS fragments might inhibit the activity of E5-TAT inside endocytic organelles. This effect could offset the gain in lytic activity observed in Figure 1 when TAT is conjugated to E5.

In addition to HS, anionic lipids represent another class of negatively charged molecules that bind to the positively charged TAT and that could affect the activity of E5-TAT inside endocytic organelles. Molecular dynamics simulations suggest that anionic groups present in the inner leaflet of a biological membrane attract TAT present on the outer leaflet of the corresponding bilayer (*72*). TAT and clustered PS on either side

of a bilayer have also been proposed to generate a local capacitor that can induce the electroporation of the membrane (*73*). It is therefore possible that TAT contributes to the lytic activity of E5-TAT by acting directly on lipid bilayers according to these proposed mechanisms. In addition, the PS asymmetry present at the plasma membrane of mammalian cells is also thought to be conserved at the membranes of endocytic organelles (*74*). In analogy to the binding observed between E5-TAT and ghosts, our data would then suggest that E5-TAT could bind to exposed PS after endosomal lysis occurs. A molecular cargo attached to E5-TAT would then remain bound to permeabilized endosomes rather than diffuse freely into the cell. This is consistent with results describing how the fluorescent protein HA2-TAT-mCherry, while being able to cause the release of a soluble dextran from endosomes into the cytosol of a cell, remains associated with endocytic organelles (*21*). Finally, the composition of the endocytic organelles is also known to change during the transition from early to late endosomes. In particular, late endosomes are enriched in the anionic lipid lysobisphosphatidic acid (LBPA) (*75*). It is therefore possible that, after trafficking within the endocytic pathway, E5-TAT might encounter a membrane leaflet more negatively charged in a late endosome than in the early endosome. Binding of the TAT moiety to LBPA could bring the E5 to the lipid bilayer. This in turn could contribute to an increase in membrane disruption by E5 in a pH-independent manner.

In conclusion, our results with RBCs provide valuable insights into the behavior of HA2-TAT peptides within endocytic organelles. From the point of view of the design of delivery agents, HA2 is employed as a pH-dependent switch that can disrupt endosomal membranes upon acidification. TAT, on the other hand, is added to the sequence to transport the HA2 moiety into the cell. Our results however highlight how the lytic activity of HA2 is profoundly affected by this addition. For E5-TAT, TAT affects the hemolytic activity, the solubility, and the binding properties of the peptide. The shifted pH response of E5-TAT in particular seems perfectly suited for delivery applications. However, TAT might also contribute to an inhibitory effect by potentially binding to HS and sequestering the peptide away from lipid bilayers. Together, these results provide the basis for the rational design of delivery agents with improved properties.

## ACKNOWLEDGMENT

We thank Professor Hayes Rye for valuable discussions. We also thank Roston Elwell, M.S. (Dept. of Mechanical Engineering), for design assistance and machining of the aluminum block apparatus.

## SUPPORTING INFORMATION AVAILABLE

Hemolysis activity of E5-TAT as a function of percent RBC in suspension and binding of Fl-E5-TAT to RBCs as function of pH. This material is available free of charge via the Internet at http://pubs.acs.org.

## REFERENCES

1. Green, M., and Loewenstein, P. M. (1988) Autonomous functional domains of chemically synthesized human immunodeficiency virus tat trans-activator protein. *Cell 55*, 1179–1188.
2. Frankel, A. D., and Pabo, C. O. (1988) Cellular uptake of the tat protein from human immunodeficiency virus. *Cell 55*, 1189–1193.
3. Wadia, J. S., and Dowdy, S. F. (2002) Protein transduction technology. *Curr. Opin. Biotechnol. 13*, 52–56.
4. Zorko, M., and Langel, U. (2005) Cell-penetrating peptides: mechanism and kinetics of cargo delivery. *Adv Drug Deliv. Rev. 57*, 529–545.
5. Duchardt, F., Fotin-Mleczek, M., Schwarz, H., Fischer, R., and Brock, R. (2007) A comprehensive model for the cellular uptake of cationic cell-penetrating peptides. *Traffic 8*, 848–866.
6. Wadia, J. S., Stan, R. V., and Dowdy, S. F. (2004) Transducible TAT-HA fusogenic peptide enhances escape of TAT-fusion proteins after lipid raft macropinocytosis. *Nat. Med. 10*, 310–315.
7. Amand, H. L., Fant, K., Norden, B., and Esbjorner, E. K. (2008) Stimulated endocytosis in penetratin uptake: effect of arginine and lysine. *Biochem. Biophys. Res. Commun. 371*, 621–625.
8. Kaplan, I. M., Wadia, J. S., and Dowdy, S. F. (2005) Cationic TAT peptide transduction domain enters cells by macropinocytosis. *J. Controlled Release 102*, 247–253.
9. Nakase, I., Tadokoro, A., Kawabata, N., Takeuchi, T., Katoh, H., Hiramoto, K., Negishi, M., Nomizu, M., Sugiura, Y., and Futaki, S. (2007) Interaction of arginine-rich peptides with membrane-associated proteoglycans is crucial for induction of actin organization and macropinocytosis. *Biochemistry 46*, 492–501.
10. Gump, J. M., June, R. K., and Dowdy, S. F. (2010) Revised role of glycosaminoglycans in TAT protein transduction domain-mediated cellular transduction. *J. Biol. Chem. 285*, 1500–1507.
11. Lee, Y. J., Datta, S., and Pellois, J. P. (2008) Real-time fluorescence detection of protein transduction into live cells. *J. Am. Chem. Soc. 130*, 2398–2399.
12. Fischer, R., Bachle, D., Fotin-Mleczek, M., Jung, G., Kalbacher, H., and Brock, R. (2006) A targeted protease substrate for a quantitative determination of protease activities in the endolysosomal pathway. *ChemBioChem 7*, 1428–1434.
13. El-Sayed, A., Futaki, S., and Harashima, H. (2009) Delivery of macromolecules using arginine-rich cell-penetrating peptides: ways to overcome endosomal entrapment. *AAPS J. 11*, 13–22.
14. Forgac, M. (2007) Vacuolar ATPases: rotary proton pumps in physiology and pathophysiology. *Nat. Rev. Mol. Cell Biol. 8*, 917–929.
15. Wharton, S. A., Martin, S. R., Ruigrok, R. W., Skehel, J. J., and Wiley, D. C. (1988) Membrane fusion by peptide analogues of influenza virus haemagglutinin. *J. Gen. Virol. 69* (Part 8), 1847–1857.
16. Smith, A. E., and Helenius, A. (2004) How viruses enter animal cells. *Science 304*, 237–242.
17. Tamm, L. K., and Han, X. (2000) Viral fusion peptides: a tool set to disrupt and connect biological membranes. *Biosci. Rep. 20*, 501–518.
18. Wagner, E., Plank, C., Zatloukal, K., Cotten, M., and Birnstiel, M. L. (1992) Influenza virus hemagglutinin HA-2 N-terminal fusogenic peptides augment gene transfer by transferrin-polylysine-DNA complexes: toward a synthetic virus-like gene-transfer vehicle. *Proc. Natl. Acad. Sci. U.S.A. 89*, 7934–7938.
19. Plank, C., Oberhauser, B., Mechtler, K., Koch, C., and Wagner, E. (1994) The influence of endosome-disruptive peptides on gene transfer using synthetic virus-like gene transfer systems. *J. Biol. Chem. 269*, 12918–12924.
20. Pichon, C., Freulon, I., Midoux, P., Mayer, R., Monsigny, M., and Roche, A. C. (1997) Cytosolic and nuclear delivery of oligonucleotides mediated by an amphiphilic anionic peptide. *Antisense Nucleic Acid Drug Dev. 7*, 335–343.
21. Lee, Y. J., Erazo-Oliveras, A., and Pellois, J. P. (2010) Delivery of macromolecules into live cells by simple co-incubation with a peptide. *ChemBioChem 11*, 325–330.
22. Koshman, Y. E., Waters, S. B., Walker, L. A., Los, T., de Tombe, P., Goldspink, P. H., and Russell, B. (2008) Delivery and visualization of proteins conjugated to quantum dots in cardiac myocytes. *J. Mol. Cell. Cardiol. 45*, 853–856.
23. Michiue, H., Tomizawa, K., Wei, F. Y., Matsushita, M., Lu, Y. F., Ichikawa, T., Tamiya, T., Date, I., and Matsui, H. (2005) The $NH_2$ terminus of influenza virus hemagglutinin-2 subunit peptides enhances the antitumor potency of polyarginine-mediated p53 protein transduction. *J. Biol. Chem. 280*, 8285–8289.
24. Thoren, P. E., Persson, D., Esbjorner, E. K., Goksor, M., Lincoln, P., and Norden, B. (2004) Membrane binding and translocation of cell-penetrating peptides. *Biochemistry 43*, 3471–3489.
25. Ciobanasu, C., Harms, E., Tunnemann, G., Cardoso, M. C., and Kubitscheck, U. (2009) Cell-penetrating HIV1 TAT peptides float on model lipid bilayers. *Biochemistry 48*, 4728–4737.
26. Esbjörner, E. K., Oglecka, K., Lincoln, P., Gräslund, A., and Nordén, B. (2007) Membrane binding of pH-sensitive influenza fusion peptides. Positioning, configuration, and induced leakage in a lipid vesicle model. *Biochemistry 46*, 13490–13504.
27. Manley, S., and Gordon, V. (2008) Making giant unilamellar vesicles via hydration of a lipid film. *Curr. Protoc. Cell Biol. 24*, 1–13.

28. Murata, M., Takahashi, S., Kagiwada, S., Suzuki, A., and Ohnishi, S. (1992) pH-dependent membrane fusion and vesiculation of phospholipid large unilamellar vesicles induced by amphiphilic anionic and cationic peptides. *Biochemistry 31*, 1986–1992.
29. Chang, D. K., Cheng, S. F., Lin, C. H., Kantchev, E. B., and Wu, C. W. (2005) Self-association of glutamic acid-rich fusion peptide analogs of influenza hemagglutinin in the membrane-mimic environments: effects of positional difference of glutamic acids on side chain ionization constant and intra- and inter-peptide interactions deduced from NMR and gel electrophoresis measurements. *Biochim. Biophys. Acta 1712*, 37–51.
30. Murata, M., Kagiwada, S., Hishida, R., Ishiguro, R., Ohnishi, S., and Takahashi, S. (1991) Modification of the N-terminus of membrane fusion-active peptides blocks the fusion activity. *Biochem. Biophys. Res. Commun. 179*, 1050–1055.
31. Mitchell, D. J., Kim, D. T., Steinman, L., Fathman, C. G., and Rothbard, J. B. (2000) Polyarginine enters cells more efficiently than other polycationic homopolymers. *J. Pept. Res. 56*, 318–325.
32. Wender, P. A., Mitchell, D. J., Pattabiraman, K., Pelkey, E. T., Steinman, L., and Rothbard, J. B. (2000) The design, synthesis, and evaluation of molecules that enable or enhance cellular uptake: peptoid molecular transporters. *Proc. Natl. Acad. Sci. U.S.A. 97*, 13003–13008.
33. Han, X., and Tamm, L. K. (2000) A host-guest system to study structure-function relationships of membrane fusion peptides. *Proc. Natl. Acad. Sci. U.S.A. 97*, 13097–13102.
34. Hsu, C. H., Wu, S. H., Chang, D. K., and Chen, C. (2002) Structural characterizations of fusion peptide analogs of influenza virus hemagglutinin. Implication of the necessity of a helix-hinge-helix motif in fusion activity. *J. Biol. Chem. 277*, 22725–22733.
35. Daniels, R. S., Downie, J. C., Hay, A. J., Knossow, M., Skehel, J. J., Wang, M. L., and Wiley, D. C. (1985) Fusion mutants of the influenza virus hemagglutinin glycoprotein. *Cell 40*, 431–439.
36. Jay, A. W., and Rowlands, S. (1975) The stages of osmotic haemolysis. *J. Physiol. 252*, 817–832.
37. Sebban, P., Coppey, M., Alpert, B., Lindqvist, L., and Jameson, D. M. (1980) Fluorescence properties of porphyrin-globin from human hemoglobin. *Photochem. Photobiol. 32*, 727–731.
38. Anderson, P. C., and Lovrien, R. E. (1977) Human red cell hemolysis rates in the subsecond to seconds range. An analysis. *Biophys. J. 20*, 181–191.
39. Boon, J. M., and Smith, B. D. (2002) Chemical control of phospholipid distribution across bilayer membranes. *Med. Res. Rev. 22*, 251–281.
40. Tiriveedhi, V., and Butko, P. (2007) A fluorescence spectroscopy study on the interactions of the TAT-PTD peptide with model lipid membranes. *Biochemistry 46*, 3888–3895.
41. Tait, J. F., Gibson, D., and Fujikawa, K. (1989) Phospholipid binding properties of human placental anticoagulant protein-I, a member of the lipocortin family. *J. Biol. Chem. 264*, 7944–7949.
42. Han, X., and Tamm, L. K. (2000) pH-dependent self-association of influenza hemagglutinin fusion peptides in lipid bilayers. *J. Mol. Biol. 304*, 953–965.
43. Jiang, T., Olson, E. S., Nguyen, Q. T., Roy, M., Jennings, P. A., and Tsien, R. Y. (2004) Tumor imaging by means of proteolytic activation of cell-penetrating peptides. *Proc. Natl. Acad. Sci. U.S.A. 101*, 17867–17872.
44. Han, X., Bushweller, J. H., Cafiso, D. S., and Tamm, L. K. (2001) Membrane structure and fusion-triggering conformational change of the fusion domain from influenza .... *Nat. Struct. Biol. 8*, 715–720.
45. Lorieau, J. L., Louis, J. M., and Bax, A. (2010) The complete influenza hemagglutinin fusion domain adopts a tight helical hairpin arrangement at the lipid:water interface. *Proc. Natl. Acad. Sci. U.S.A. 107*, 11341–11346.
46. Harris, T. K., and Turner, G. J. (2002) Structural basis of perturbed pKa values of catalytic groups in enzyme active sites. *IUBMB Life 53*, 85–98.
47. Zhelev, D. V., Stoicheva, N., Scherrer, P., and Needham, D. (2001) Interaction of synthetic HA2 influenza fusion peptide analog with model membranes. *Biophys. J. 81*, 285–304.
48. Lieber, M. R., and Steck, T. L. (1982) A description of the holes in human erythrocyte membrane ghosts. *J. Biol. Chem. 257*, 11651–11659.
49. Hoffman, J. F. (1992) On red blood cells, hemolysis and resealed ghosts. *Adv. Exp. Med. Biol. 326*, 1–15.
50. Mellman, I. (1996) Endocytosis and molecular sorting. *Annu. Rev. Cell Dev. Biol. 12*, 575–625.
51. Schmid, S., Fuchs, R., Kielian, M., Helenius, A., and Mellman, I. (1989) Acidification of endosome subpopulations in wild-type Chinese hamster ovary cells and temperature-sensitive acidification-defective mutants. *J. Cell Biol. 108*, 1291–1300.
52. Demaurex, N. (2002) pH homeostasis of cellular organelles. *News Physiol. Sci. 17*, 1–5.
53. Tyagi, M., Rusnati, M., Presta, M., and Giacca, M. (2001) Internalization of HIV-1 tat requires cell surface heparan sulfate proteoglycans. *J. Biol. Chem. 276*, 3254–3261.
54. Console, S., Marty, C., Garcia-Echeverria, C., Schwendener, R., and Ballmer-Hofer, K. (2003) Antennapedia and HIV transactivator of transcription (TAT) "protein transduction domains" promote endocytosis of high molecular weight cargo upon binding to cell surface glycosaminoglycans. *J. Biol. Chem. 278*, 35109–35114.
55. Poon, G. M., and Gariepy, J. (2007) Cell-surface proteoglycans as molecular portals for cationic peptide and polymer entry into cells. *Biochem. Soc. Trans. 35*, 788–793.
56. Hakansson, S., Jacobs, A., and Caffrey, M. (2001) Heparin binding by the HIV-1 tat protein transduction domain. *Protein Sci. 10*, 2138–2139.
57. Hakansson, S., and Caffrey, M. (2003) Structural and dynamic properties of the HIV-1 tat transduction domain in the free and heparin-bound states. *Biochemistry 42*, 8999–9006.
58. Rusnati, M., Coltrini, D., Oreste, P., Zoppetti, G., Albini, A., Noonan, D., d'Adda di Fagagna, F., Giacca, M., and Presta, M. (1997) Interaction of HIV-1 Tat protein with heparin. Role of the backbone structure, sulfation, and size. *J. Biol. Chem. 272*, 11313–11320.
59. Richard, J. P., Melikov, K., Brooks, H., Prevot, P., Lebleu, B., and Chernomordik, L. V. (2005) Cellular uptake of unconjugated TAT peptide involves clathrin-dependent endocytosis and heparan sulfate receptors. *J. Biol. Chem. 280*, 15300–15306.
60. Silhol, M., Tyagi, M., Giacca, M., Lebleu, B., and Vives, E. (2002) Different mechanisms for cellular internalization of the HIV-1 Tat-derived cell penetrating peptide and recombinant proteins fused to Tat. *Eur. J. Biochem. 269*, 494–501.
61. Violini, S., Sharma, V., Prior, J. L., Dyszlewski, M., and Piwnica-Worms, D. (2002) Evidence for a plasma membrane-mediated permeability barrier to Tat basic domain in well-differentiated epithelial cells: lack of correlation with heparan sulfate. *Biochemistry 41*, 12652–12661.
62. Fuchs, S. M., and Raines, R. T. (2006) Internalization of cationic peptides: the road less (or more?) traveled. *Cell. Mol. Life Sci. 63*, 1819–1822.
63. Kosuge, M., Takeuchi, T., Nakase, I., Jones, A. T., and Futaki, S. (2008) Cellular internalization and distribution of arginine-rich peptides as a function of extracellular peptide concentration, serum, and plasma membrane associated proteoglycans. *Bioconjugate Chem. 19*, 656–664.
64. Wittrup, A., Zhang, S. H., ten Dam, G. B., van Kuppevelt, T. H., Bengtson, P., Johansson, M., Welch, J., Morgelin, M., and Belting, M. (2009) ScFv antibody-induced translocation of cell-surface heparan sulfate proteoglycan to endocytic vesicles: evidence for heparan sulfate epitope specificity and role of both syndecan and glypican. *J. Biol. Chem. 284*, 32959–32967.
65. Fischer, R., Fotin-Mleczek, M., Hufnagel, H., and Brock, R. (2005) Break on through to the other side-biophysics and cell biology shed light on cell-penetrating peptides. *ChemBioChem 6*, 2126–2142.
66. Yanagishita, M., and Hascall, V. C. (1984) Metabolism of proteoglycans in rat ovarian granulosa cell culture. Multiple intracellular degradative pathways and the effect of chloroquine. *J. Biol. Chem. 259*, 10270–10283.
67. Brauker, J. H., and Wang, J. L. (1987) Nonlysosomal processing of cell-surface heparan sulfate proteoglycans. Studies of I-cells and NH4Cl-treated normal cells. *J. Biol. Chem. 262*, 13093–13101.
68. Bame, K. J. (1993) Release of heparan sulfate glycosaminoglycans from proteoglycans in Chinese hamster ovary cells does not require proteolysis of the core protein. *J. Biol. Chem. 268*, 19956–19964.
69. Egeberg, M., Kjeken, R., Kolset, S. O., Berg, T., and Prydz, K. (2001) Internalization and stepwise degradation of heparan sulfate proteoglycans in rat hepatocytes. *Biochim. Biophys. Acta 1541*, 135–149.
70. Drzeniek, Z., Stocker, G., Siebertz, B., Just, U., Schroeder, T., Ostertag, W., and Haubeck, H. D. (1999) Heparan sulfate proteoglycan expression is induced during early erythroid differentiation of multipotent hematopoietic stem cells. *Blood 93*, 2884–2897.

71. Vogt, A. M., Winter, G., Wahlgren, M., and Spillmann, D. (2004) Heparan sulphate identified on human erythrocytes: a *Plasmodium falciparum* receptor. *Biochem. J. 381*, 593–597.
72. Herce, H. D., and Garcia, A. E. (2007) Molecular dynamics simulations suggest a mechanism for translocation of the HIV-1 TAT peptide across lipid membranes. *Proc. Natl. Acad. Sci. U.S.A. 104*, 20805–20810.
73. Cahill, K. (2009) Molecular electroporation and the transduction of oligoarginines. *Phys. Biol. 7*, 16001.
74. van Meer, G., Voelker, D. R., and Feigenson, G. W. (2008) Membrane lipids: where they are and how they behave. *Nat. Rev. Mol. Cell Biol. 9*, 112–124.
75. Kobayashi, T., Beuchat, M. H., Chevallier, J., Makino, A., Mayran, N., Escola, J. M., Lebrand, C., Cosson, P., and Gruenberg, J. (2002) Separation and characterization of late endosomal membrane domains. *J. Biol. Chem. 277*, 32157–32164.